Supplementary Materials.

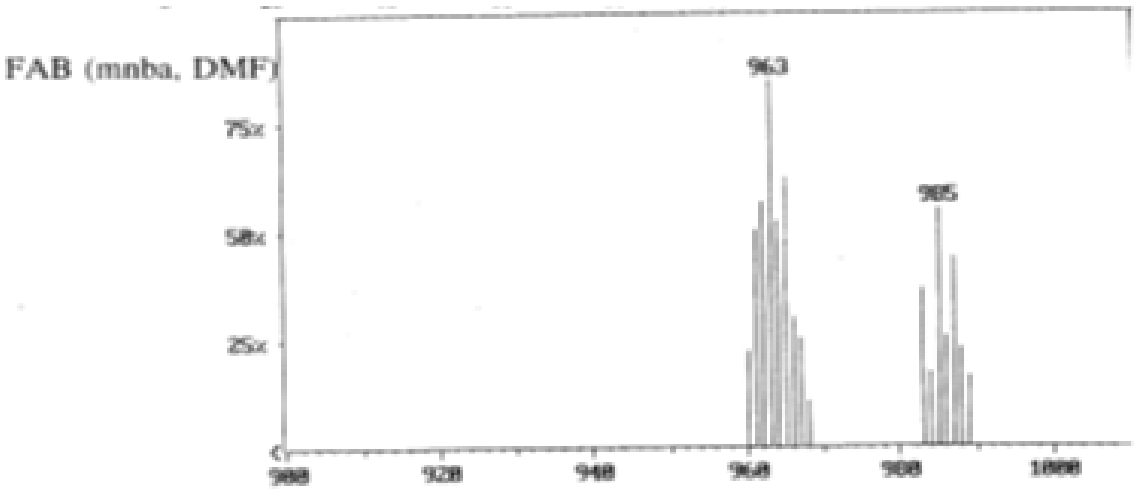

Figure S1. Experimental FAB spectrum (DMSO, mnba matrix) for the $(L^7HCu)_2Zn{\cdot}2CH_3OH$ complex**.**

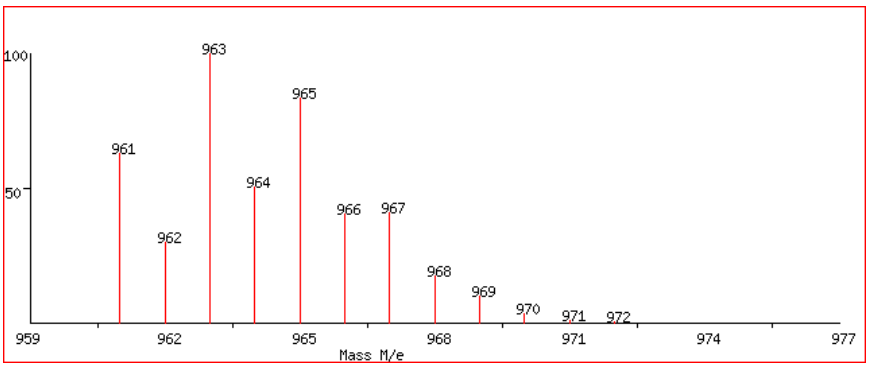

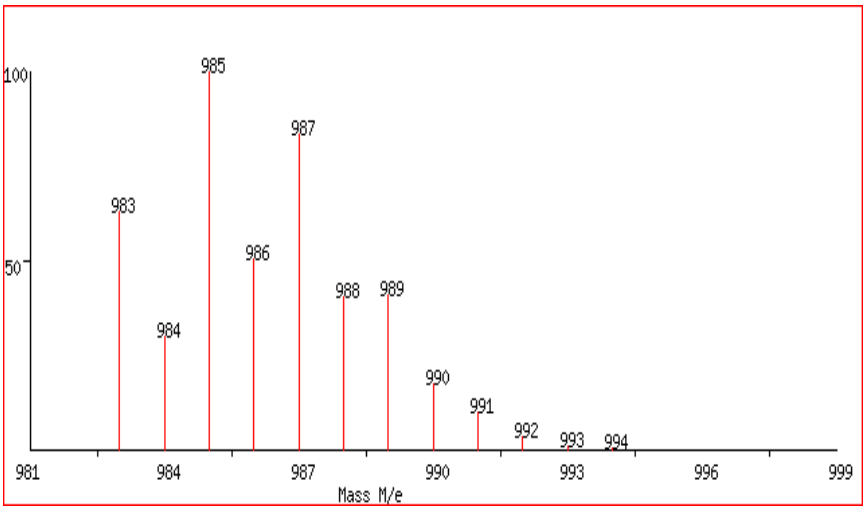

Figure S2. Theoretical isotopic distribution for the $[(L^7HCu)_2Zn +1]^+$ and the $[(L^7HCu)_2Zn + Na]^+$ monocationic species.

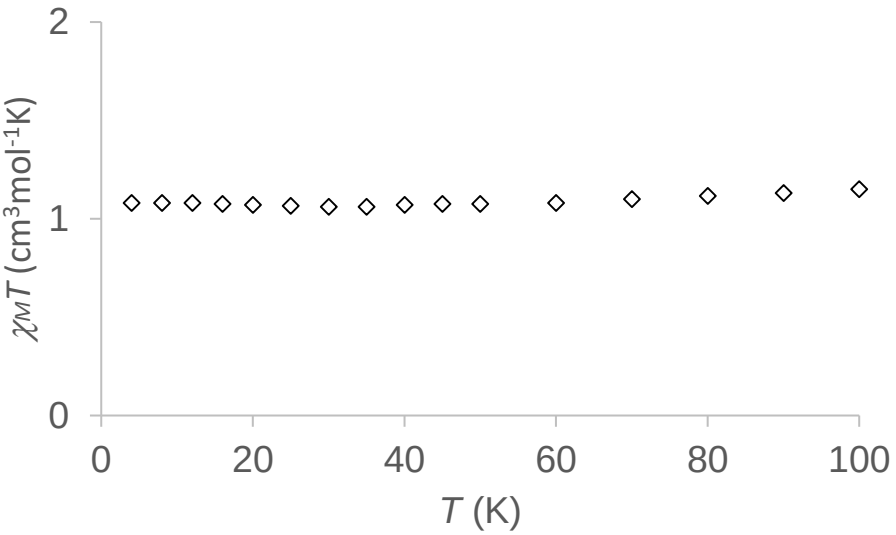

Figure S3. Temperature dependence of the $\chi_M T$ product for $(L^7HCu)_2VO{\cdot}2CH_3OH$ at 0.1 T applied magnetic field.

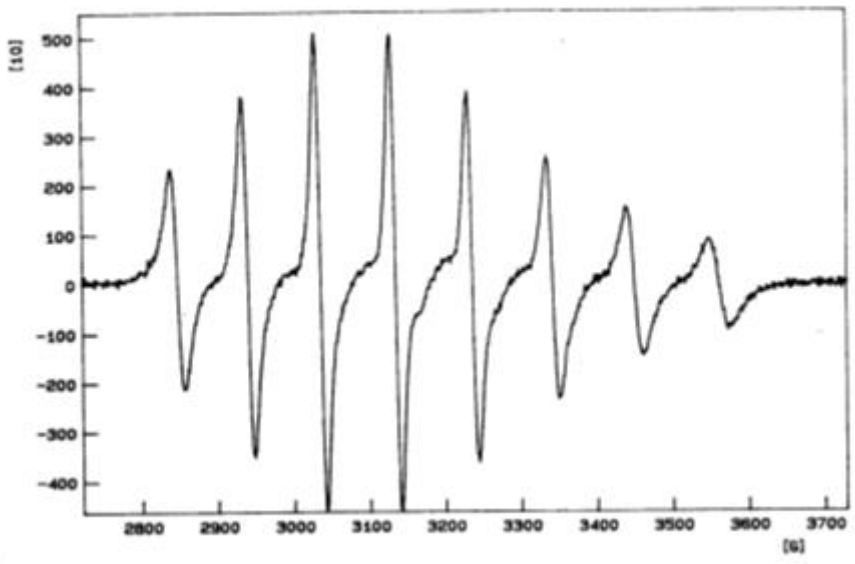

Figure S4. EPR spectrum for the $NiL^{3}VO$ complex at room temperature and CH_2Cl_2 solvent.

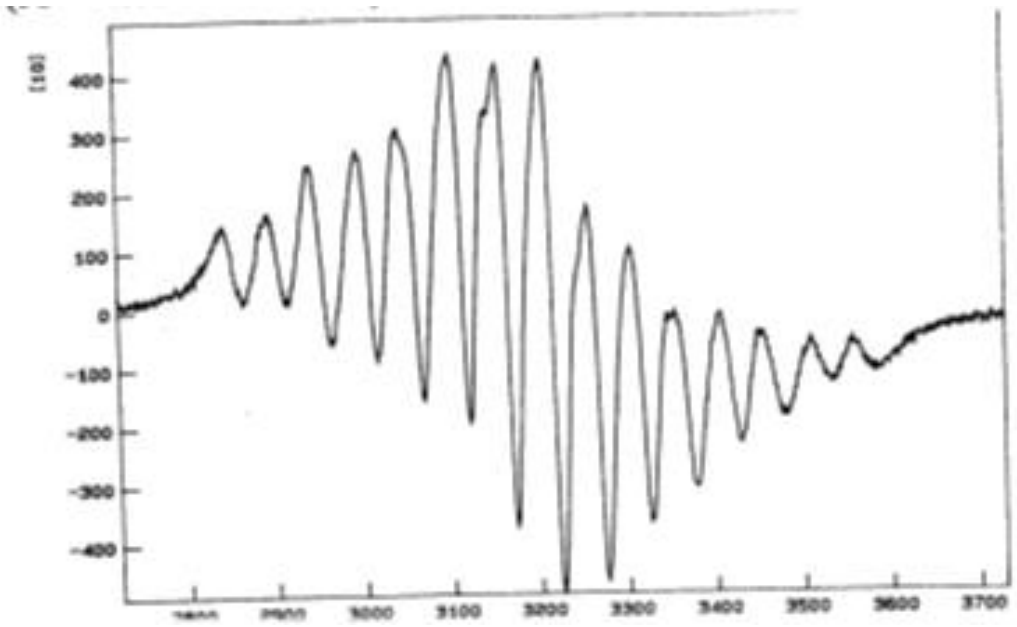

Figure S5. EPR spectrum for the $VOL^{3}VO$ conformers at room temperature and CH_2Cl_2 solvent.

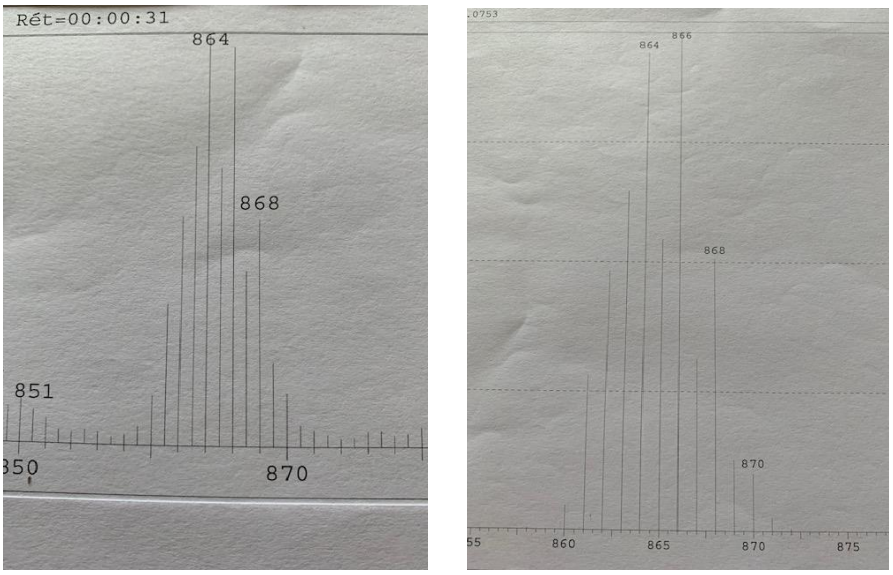

Figure S6. Experimental FAB spectrum (DMSO, mnba matrix) (left) and theoretical spectrum (right) for the $(L^2Cu)_2Gd(NO_3)_3 \cdot 5H_2O$ complex.

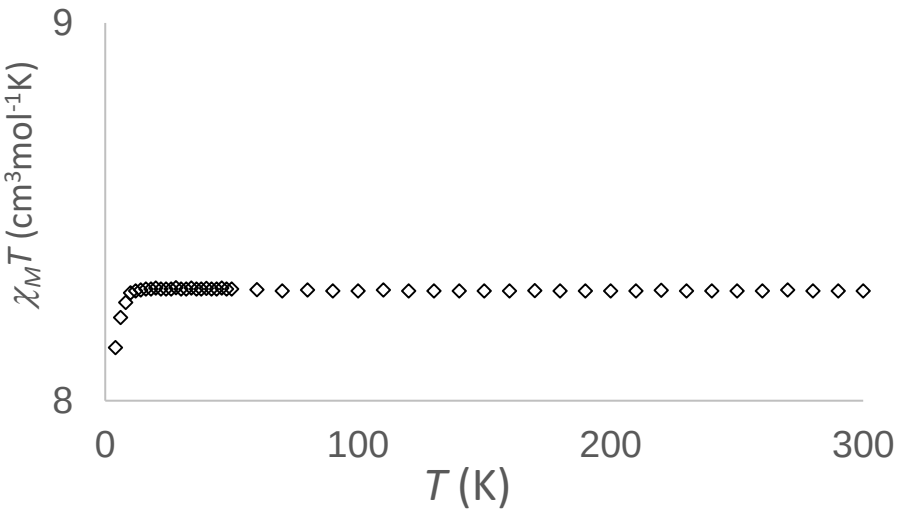

Figure S7. Temperature dependence of the $\chi_M T$ product for $(L^2Cu)_2Gd(NO_3)_3 \cdot 5H_2O$ at 0.1 T applied magnetic field.

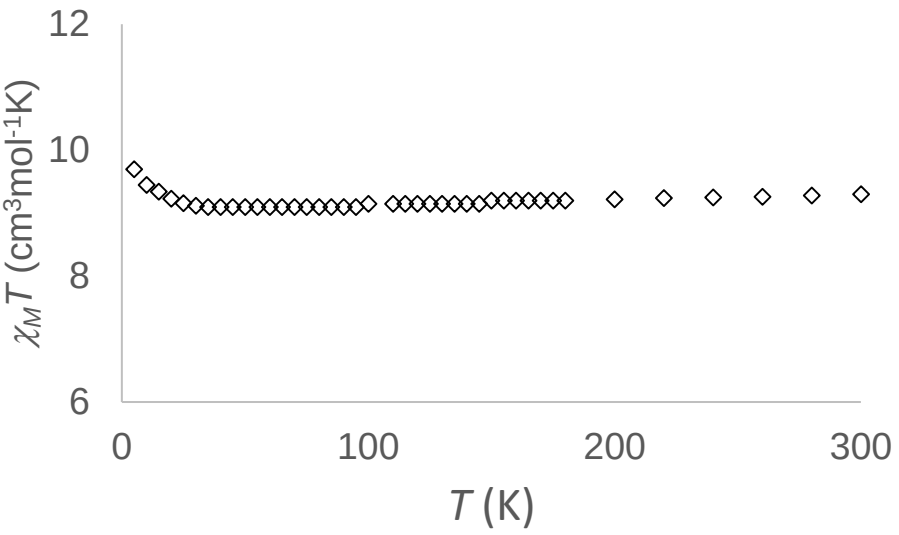

Figure S8. Temperature dependence of the $\chi_M T$ product for $(L^5Cu)_3Gd \cdot 5H_2O$ at 0.1 T applied magnetic field.